

3. Power system aggregation

In the former chapter necessity of modeling induction motor load and load branch. Assuming to model the two, it is evident that some improvement must be introduced to today's power system aggregation technique, because today's aggregated power system model does not include load branch.

Ref (1) in 1979 said frankly that "Around these problems around power system aggregation, various researches are vigorously performed, many papers are published, but no methodology is established yet. In the committee some examination is performed, but ultimate conclusion was not obtained." Some technical progresses appeared afterward. Here, History of aggregation is introduced meta-theoretically

Coherency based and Eigenvalue based

Modern aggregation methods are divided into two kinds, that is, *Coherency Based* and *Eigenvalue Based*. In the end of 20th century the two methods held serious controversy in US.

Coherency Based method identifies coherent groups where generators swing coherently by assuming some fault, aggregate each coherent group into one machine and one load. The method can be certainly practiced., however, accuracy of its result is not necessarily insured. In addition Ref. (2) pointed out that inadequate fault point will cause inadequate coherent groups. However, although the method has problem in accuracy, it can be verified by case studies, the method can be anyhow achieved and can be summed up to program, thus the method is currently the main practical stream.

Eigenvalue Based method preserves slow and ill convergent eigenvalue, and therefore, can make aggregated model without assuming some fault. For the problem that a large amount of calculation is needed, Ref. (3) proposes countermeasure. As to the method how distinct ignorable eigenvalue, Ref. (4) presents a solution. Although eigenvalues that should be preserved are identified, methodology to synthesize aggregated model using parts used in conventional analyses. As to the point Ref. (5) proposes a solution. However totally saying, the method is promising in accuracy, but as the final difficulty, that is, general methodology for building up objective aggregated model is not established, so does not penetrate in practical use.

In US, developed aggregation programs such as DYNEQU and DYNRED are applied to existing power systems and the results are published as (6) and (7). These achievements rarely seen in Japan. However even in US, most research of aggregation treat load as simple impedance, although load's dynamic character is generally noticed as fatally important in power system analyses. Among them, it must be noticed that Kunder pointed out that load's dynamic character must be considered when identifying coherent groups, in discussion of Ref. (8) and (9).

Network aggregation and generator aggregation

Today's main stream is *Coherency Based* method. Although systematic methodology is not established in the first step of identifying coherent groups, which is evident from experienced engineer's point of view. Local system interconnected via high impedance transformer is typical as an example.

Aggregation coherent group to one machine one load as the second step is classified into network aggregation and generator aggregation. Aggregation of generators themselves is achieved without problem, but methodology of aggregating excitation systems and speed governing systems. Typical simulation tool in Japan takes a rough method that represents aggregated excitation and speed governing systems by those of the largest generator included object system. Since the largest generator must be modern and high spec, performance of the aggregated system must be

superior than reality. Although programming is still not established, Ref. (10) proposes to maintain frequency response, ceiling voltage, and response time in excitation system aggregation.

What can be now evaluated is only network aggregation error. For the purpose some means are needed like that generators, excitation systems, and speed governing systems should be replaced to those of standard character.

Two element method and three element method

Network aggregation can be describe as these two stage as follows, considering it as matter of course that generators' capacity and output, loads' active and reactive power are preserved through aggregation.

First step: Assume structure of aggregated system. Researches up to now assume one of the two structures shown in Fig. 3.1. Old researches adopt (a) two-element methods with two freedom. In 2002 Ref. (11) proposed "Y-connection method", one of (b) three-element methods with three freedom. Z_{SL} represents load branch introduced in the former chapter.

Second step: Select variables that are preserved through aggregation. Selected same number of variable as freedom, two impedances in two-element method or three impedances in three-element method can be calculated uniquely.

Selection of variables to be preserved generates various aggregation methods. These as follows are considered as variables to be preserved⁽³⁰⁾.

- 1) Z_G : Impedance from aggregation point to generator(s).
- 2) Z_L : Impedance from aggregation point to load(s)
- 3) V_L : Load voltage during fault
- 4) Active and reactive power loss
- 5) θ_G : Angle of generator terminal from aggregation point. This is approximately calculated as $\theta_G = \sum (X P)$, that is, accumulated product of reactance X and power P on route from aggregation point to generator.

$A_G = \sum (Z P)$, using impedance Z with real part instead of jX , is named "complex angle", and is an extended concept of angle.

- 6) θ_L : Angle of load terminal from aggregation point. Complex angle A_L is defined as an extended concept of θ_L .

Among variables to be preserved, Z_G rules short circuit current and power swing period, therefore, is indispensable. Also generator angle θ_G (A_G) should have priority than load angle θ_L (A_L).

In two-element methods except two-load method preserving active and reactive loss is difficult, so adjusted by increasing load. These methods as follows are possible, and their characters are introduced.

(a) $Z_G Z_L$ method: Voltage stability may be preserved, because impedance to load is preserved. However, negative impedance often appears. In such cases, commercial tool changes impedances as $Z_S : Z_{SG} = 9 : 1$ without concrete reasons.

(b) $Z_G V_L$ method: Transient stability may be preserved, because voltage and power of load during fault is

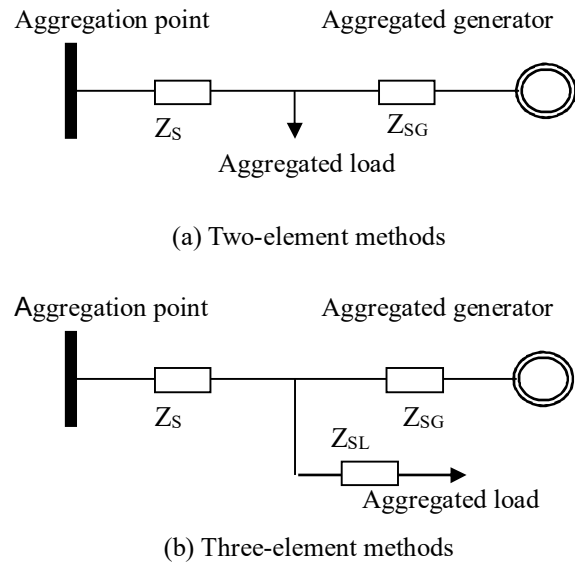


Fig. 3.1 Structure that network aggregation assumes

preserved.

(c) $Z_G A_G$ method: Transient stability may be preserved, because generator terminal angle at initial condition is preserved.

(d) Two-load method⁽¹³⁾: The method is one of two-element methods, but a part of load is located at aggregation point or generator terminal. Since dividing ratio of active and reactive load power can be chosen freely, loss is also preserved as one more variable to be preserved in the method, which can be called as “ $Z_G A_G$ Loss method”. However considering loss in load branch, negative load sometimes appears.

No example preserving V_L is seen in three-element method. Two methods as follows were proposed.

(e) $Z_G A_G Z_L$ method: Transient and voltage stability may be preserved. As result, loss and voltage drop (rise) are well reserved in most cases.

(f) $Z_G A_G A_L$ method: Transient and voltage stability may be preserved. As result, preservation loss and voltage drop (rise) is approximately proven.

Accuracy of network aggregation is superior in three-element methods than two-element methods, because number preserved variables is larger. Especially when induction motor load or load branch is modeled in detailed system, accuracy is kept better in three-element method⁽¹²⁾. Since load model and aggregation relate closely, unified research of the two is necessary and it has already begun⁽¹²⁾.

Proof on preserving loss and voltage in Y-connection method

In $Z_G A_G A_L$ (Y-connection) method, active and reactive loss is approximately preserved. Here, it is proved.

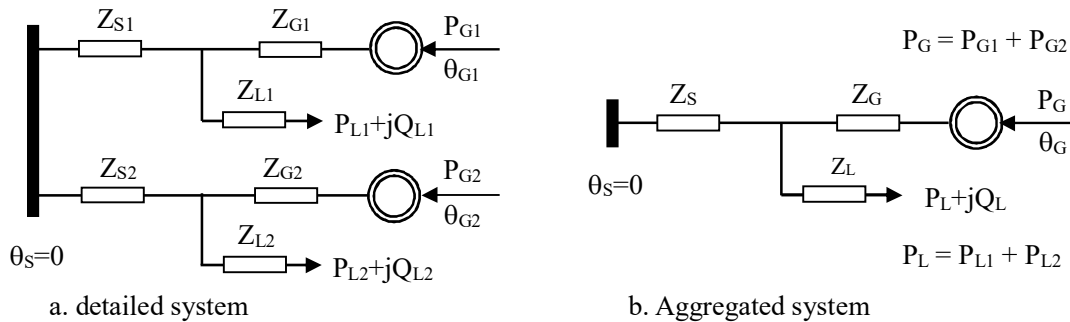


Fig. 3.2 Impedance and power flow of object system.

Two subsystem connect to common bus are assumed as Fig. 3.2a. The two are aggregated as Fig. 3.2b. Here, complex angle θ is introduced. This is accumulated product of impedance Z and power flow P from trunk bus to the point in question, and is expressed as follows.

$$\theta = \Sigma (ZP)$$

Equations of power flow concerning to complex angle are expressed as follows.

$$\theta_{G1} = Z_{S1} (P_{G1} - P_{L1}) + Z_{G1} P_{G1}$$

$$\theta_{L1} = Z_{S1} (P_{G1} - P_{L1}) - Z_{L1} P_{L1}$$

$$\theta_{G2} = Z_{S2} (P_{G2} - P_{L2}) + Z_{G2} P_{G2}$$

$$\theta_{L2} = Z_{S2} (P_{G2} - P_{L2}) - Z_{L2} P_{L2} \quad (3.1)$$

$$\theta_G = Z_S (P_{G1} + P_{G2} - P_{L1} - P_{L2}) + Z_G (P_{G1} + P_{G2})$$

$$\theta_L = Z_S (P_{g1} + P_{g2} - P_{L1} - P_{L2}) - Z_L (P_{L1} + P_{L2})$$

Since kW weighted complex angle is preserved, relations as follows are conducted.

$$\begin{aligned} (P_{G1} + P_{G2}) \theta_G &= P_{G1} \theta_{G1} + P_{G2} \theta_{G2} \\ (P_{L1} + P_{L2}) \theta_L &= P_{L1} \theta_{L1} + P_{L2} \theta_{L2} \end{aligned} \quad (3.2)$$

From eq. (3.1) and eq. (3.2), equation as follows is conducted.

$$\begin{aligned} &(P_{G1} + P_{G2}) \theta_G - (P_{L1} + P_{L2}) \theta_L \\ &= Z_S (P_{G1} + P_{G2} - P_{L1} - P_{L2})^2 + Z_G (P_{G1} + P_{G2})^2 + Z_L (P_{L1} + P_{L2})^2 \\ &= P_{G1} \theta_{G1} + P_{G2} \theta_{G2} - P_{L1} \theta_{L1} - P_{L2} \theta_{L2} \\ &= Z_{S1} (P_{G1} - P_{L1})^2 + Z_{G1} P_{G1}^2 + Z_{L1} P_{L1}^2 \\ &\quad + Z_{S2} (P_{G2} - P_{L2})^2 + Z_{G2} P_{G2}^2 + Z_{L2} P_{L2}^2 \end{aligned} \quad (3.3)$$

Eq. (3.3) means that active and reactive power loss on branches is equal in detailed system and aggregated system. Repeating the process, every radial system can be aggregated into one machine one load form as Fig. 3.3b. As internal impedance of generator, direct axis transient reactance X_d' is suitable, because it has an important role in power system analyses. Assumed all generators have 30% X_d' in machine capacity base (the assumption has considerable reality), Y-connection method does not need except system impedance and power flow. That is a practically convenient character.

Y-connection method also approximately preserves voltage rise(for generator)/drop(for load). This is also proven. Impedance of branch #i: Z_i is constructed by resistance R_i and reactance X_i as follows.

$$Z_i = R_i + j X_i$$

It is supposed that reactive power flow Q_i is proportional to active power flow P_i in all branches as follows. Taking whole view, the assumption is not so doubtful.

$$Q_i = A P_i \quad (3.4)$$

Then, complex angle is expressed as follows.

$$\theta = \Sigma \{ (R_i + j X_i) P_i \} = \Sigma(R_i P_i) + j \Sigma(X_i P_i)$$

Of course weighted average of real part $\Sigma (R_i P_i)$ and imaginary part $\Sigma (X_i P_i)$ are preserved independently. While assumption of eq. (3.4) exists, weighted average of $\Sigma (X_i Q_i)$ is also preserved. That is well known equation of approximate voltage rise/drop itself.

Aggregation of loop system

Ref. (14) points out two items to be considered in local system aggregation. One is voltage support by reactive supply from local generators. Another is bypassed power flow to local system paralleled with trunk system.

Ref. (10) proposes a structure of loop aggregated system having one more aggregation point 2 as shown in Fig. 3.3.

Aggregation point is connected to some point on either one branch of the three. Thus five branches to be identified appear in aggregated system on one hand.

On the other hand there are six variables that are hoped to be preserved as follows.

- 1) Z_G : Impedance from aggregation point 1 to generator
- 2) Z_{G2} : Impedance from aggregation point 2 to generator
- 3) Z_{LOOP} : Impedance from aggregation point 1 to point 2
- 4) A_G : Complex angle of generator
- 5) A_L : Complex angle of load
- 6) A_2 : Complex angle of aggregation point 2

Among the six, one must be given up being preserved. (3) to (6) are indispensable for preserving power flow. Therefore among (1) and (2), less important (2) should be given up. As the result, accuracy of aggregation of loop system is inferior to that of radial system. However, the accuracy is applicable in practical use, although it is not published yet.

A new interpretation of two-load method

Traditional interpretation of two-load method is that a part of aggregated load shifted to aggregation point or generator terminal. Therefore, two kinds exist. Here, the former is called as two-load-S method, and the latter is as two-load -G method. Two-load method is smart because network loss is preserved by using additional variable: load dividing ratio.

However, faithfully built power system models have load branches from bus to load, and loss in load branch is not ignorable. For considering the loss on load branches, negative load often appears by two-load method. This is understood by a new interpretation as follows.

That is, besides real load P_L , imaginary load P_L' and $-P_L'$ are put as shown in Fig. 3.4, and imaginary power flow P_L' shown gray arrows in the figure are piled up. Of course the imaginary power flow is used for only adjusting initial power flow, so their dynamic character can be neglected, and modeled as constant impedance.

(a) Suppose two-load-S method. When detailed system

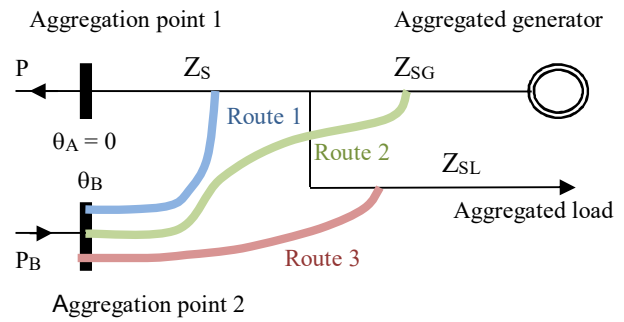


Fig. 3.3 Aggregation of loop system with two interconnections

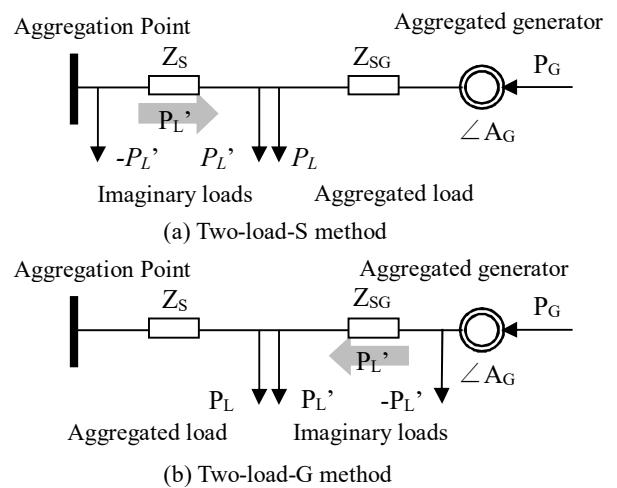


Fig. 3.4 Structure assumed by two-load method

with load branch is aggregated by two-load-S method, imaginary power flow P_L' from aggregation point to load is piled up. Here, impedance from aggregation point to generator $Z = Z_S + Z_{SG}$ is preserved, and also complex angle of generator before piling up the imaginary power flow is preserved. If system side impedance when imaginary power flow $P_L' > 0$ is piled up is calculated as Z_S' relationship as follows is conducted.

$$A_G = P_G Z - (P_L + P_L') Z_S'$$

From these relationships, equation as follows is conducted.

$$Z_S' / Z_S = P_L / (P_L + P_L')$$

Therefore, $Z_S' < Z_S$.

Increased loss by piling up the imaginary power flow is calculated as follows.

$$\Delta P + j\Delta Q = Z_S' (P_L + P_L' - P_G)^2 + (Z - Z_S') P_G^2 - Z_S (P_L - P_G)^2 - (Z - Z_S) P_G^2 = Z_S P_L P_L' > 0$$

Network loss increases by piling up the imaginary power flow $P_L' > 0$.

(b) Suppose two-load-G method. If generator side impedance when imaginary power flow $P_L' > 0$ is piled up is calculated as Z_{SG}' relationship as follows is conducted.

$$Z_{SG}' / Z_{SG} = P_L / (P_L + P_L')$$

Therefore, $Z_{SG}' < Z_{SG}$, as the result, $Z_S' > Z_S$.

Increased loss by piling up the imaginary power flow is calculated as follows.

$$\Delta P + j\Delta Q = (Z - Z_{SG}') (P_G - P_L)^2 + Z_{SG}' (P_G + P_L')^2 - (Z - Z_{SG}) (P_G - P_L)^2 - Z_{SG} P_G^2 = Z_S P_L P_L' > 0$$

Network loss increases by piling up the imaginary power flow $P_L' > 0$.

In case of modeling induction motor load, impedance $Z_S + Z_{SL}$ must reflect the reality. Aggregating by three-element method, Z_{SL} takes a large value. Therefore by study up to here, value order of $Z_S + Z_{SL}$ is expressed as follows.

Two-load-S method < two-element method < two-load-G method < tree-element method

Assuming that three-element method reflects the reality, accuracy of two-load-G method is slightly inferior, that of two-element method is inferior more, and that of two-load-S method is inferior most. Among the two two-load methods, two-load-S method reflects load distribution of detailed system better, but two-load-G method reflects impedance from aggregation point to induction motor load better.

Merit of two-load method is that network loss is preserved by introducing additional variable: load dividing ratio, although structure is still two-element method. However, preservation of loss can be realized also by three-element methods. Even in case of two-element method, additional loss on load branch $\Delta P_L + j\Delta Q_L$ calculated by DC flow method can be added to real load, and similar effect as two-load methods can be realized.

In aggregation accuracy, two-load-S method is inferior to two-element method, and two-load-G method is superior to two-element method. Two-load method are not always superior to two-element methods. Thus, merit of two-load methods is not absolute. The limit of two-load method is derived from neglect in structure of load branch certainly existing in real system. Therefore as effective breakthrough, nothing but adopting three-element method

that models load branch in structure.

Thus, various network aggregation methods are introduced by meta-theoretical way, two-load methods are closed up and their merit and limitation are discussed. Aggregation accuracy of four types when induction motor load is modeled is only qualitatively guessed. Three-element method is superior. But quantitative accuracy assessment is not done yet. Here, it is performed by simulation on a local example system.

Assessment of two-load method

Since two-load method is a network aggregation methods, aggregation of generator and control system is not dealt. In trunk system various generators and control system are mixed, so network aggregation accuracy cannot be assessed. Local system with only hydro generation is suitable. Existing 66kV class local system is introduced in Fig. 3.5 and Table 3.1. Load power far exceeds generated power, that is, power receiving system.

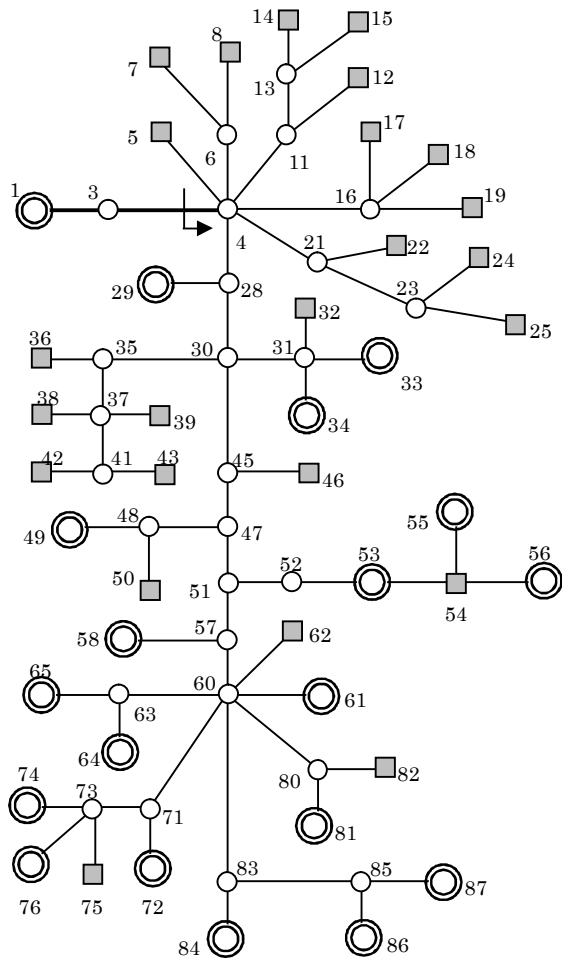


Fig. 3.5 Structure of the example local system

Table 3.1 Impedance and power flow condition of example sys.

FROM	TO	R	X	PG(TO)	PL(TO)	WG(TO)
0	1	0	0			
1	2	0	0	0	0	0
1	3	0.2262	0			
3	4	0.2731	0			
4	5	3.0243	6.0962		0.01	
4	6	0.02885	0.2403			
6	7	0.745607	4.025999		0.041	
6	8	0.834761	4.288204		0.037	
4	11	0.01165	0.09735			
11	12	0.681968	3.808692		0.044	
11	13	0.01505	0.1249			
13	14	0.454545	3.324309		0.066	
13	15	0.7827	15.23698		0.003	
4	16	0.0279	0.32385			
16	17	0.681818	4.985348		0.044	
16	18	1.00735	5.81405		0.03	
16	19	0.691168	1.528281		0.044	
4	21	0.00665	0.05585			
21	22	0.0067	6.623091		0.006	
21	23	0.02225	0.19225			
23	24	0.982592	4.495126		0.031	
23	25	2.52735	8.788857		0.012	
4	28	0.01975	0.12525			
28	29	0.0344	15.1422	0.0033		0.0052
28	30	0.03995	0.10485			
30	31	0	3.75021			
31	32	1.153846	2.307692		0.026	
31	33	3.489	21.073	0.0011		0.0019
31	34	15.991	18.3815	0.001		0.0019
30	35	0.01285	0.1092			
35	36	0.0557	12.89373		0.006	
35	37	0.0129	0.10795			
37	38	0.007	3.926355		0.018	
37	39	0.001	5.612711		0.018	
37	41	0.0246	0.1195			
41	42	0.0007	4.212075		0.018	
41	43	1.01075	4.462526		0.03	
30	45	0.0148	0.1264			
45	46	0.0103	11.04714		0.007	
45	47	0.00845	0.07295			
47	48	0.0048	0.0112			
48	49	0	1.54	0.0027		0.0045
48	50	6	19.44		0.005	
47	51	0.0273	0.2299			
51	52	0.0007	0.0017			
52	53	0	7.75	0.004		0.007
53	54	7.5	15		0.004	
54	55	33.77	103.12	0.0008		0.0012
54	56	13.68	40.41	0.0008		0.0015
51	57	0.0051	0.0439			
57	58	0.2402	17.0685	0.0106		0.0168
57	60	0.0235	0.2005			
60	61	0	7.14	0.0093		0.014
60	62	4.285714	16.28143		0.007	
60	63	0.0771	0.2734			
63	64	0	7.5	0.0063		0.01
63	65	0.4216	31.453	0.0022		0.0033
60	71	0.2097	0.6686			
71	72	0.0246	7.3998	0.0053		0.0085
71	73	0.286	0.7364			
73	74	0	7.516	0.0099		0.017
73	75	10	28.717		0.003	
73	76	0.2799	29.8238	0.0043		0.007
60	80	0.2181	0.5736			
80	81	0	4.865	0.0127		0.0196
80	82	7.5	30.15		0.004	
60	83	0.2524	0.7654			
83	84	0.0035	21.0073	0.0021		0.0035
83	85	0.0143	0.0799			
85	86	0.0043	2.8571	0.0216		0.0316
85	87	0.1074	5.162429	0.0091		0.0147

Generator constants are assumed as typical values of small hydro generator as Table 3.2. Exciting system is also assumed as typical design as Fig. 3.6. Speed governing system is locked by assuming level governor operation.

Table 3.2 Constants of the hydro generators

M	Xd	Xd'	Xd''	Td'	Td''	Xq	Xq''	Tq''	Xl	Ta
5.0	1.15	0.3	0.22	1.2	0.03	0.75	0.22	0.03	0.18	0.3
Saturation		Ea	0.5	0.8	1.0	1.1	1.2			
If		0.5	0.85	1.15	1.35	1.75				

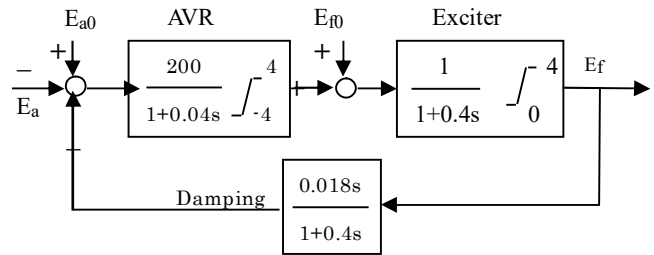


Fig. 3.6 Excitation system of the hydro generators

In case of induction motor load model, motor ratio (motor consumption power/load consumption power) is chosen as 50%, loading (consumption power kW/capacity kVA) is chosen as 50%, and unit inertia constants is chosen as 0.5 sec.

In case of static load model, load's active and reactive power P, Q are assumed to be decided only by instant voltage V and frequency f as follows.

$$P \propto V^1 f^2, Q \propto V^2$$

And it is assumed that static load turns to constant impedance at 70% voltage or lower.

Impedances and power flows of aggregated systems by the four method are shown in Table 3.3. Certainly order of $Z_S + Z_{SL}$ value of is same of theory as follows.

Table 3.3 Impedance and flow of example aggregated system

Method	Z_S	Z_{SG}	Z_{SL}		
2E	0.01888+j0.09000	0.14188+j1.38536	0		
2L-S	0.00298+j0.01893	0.22784+j1.44643	0		
2L-G	0.04687+j0.29754	0.18396+j1.16782	0		
3E	0.01888+j0.09000	0.14188+j1.38536	0.04003+j0.258066		
Method	P _G	P _L	ΔP_L	ΔQ_L	P _{L'}
2E	0.1071	0.514	0.0153	0.0973	0
2L-S	0.1071	0.514	0	0	1.6581
2L-G	0.1071	0.514	0	0	0.0957
3E	0.1071	0.514	0	0	0

Two-load-S method < two-element method < two-load-G method < tree-element method

As failure 3φG – 0.1sec – clear is modeled at aggregation point. Simulation result are shown by downward power flow at aggregation point. Induction motor load case is shown in Fig. 3.7. Static load case in Fig. 3.8.

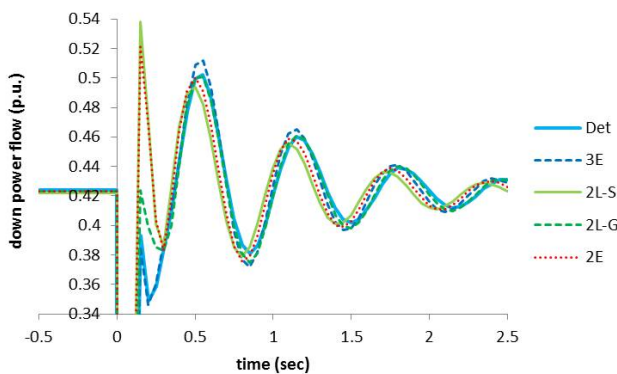


Fig. 3.7 Aggregation accuracy (induction motor load)

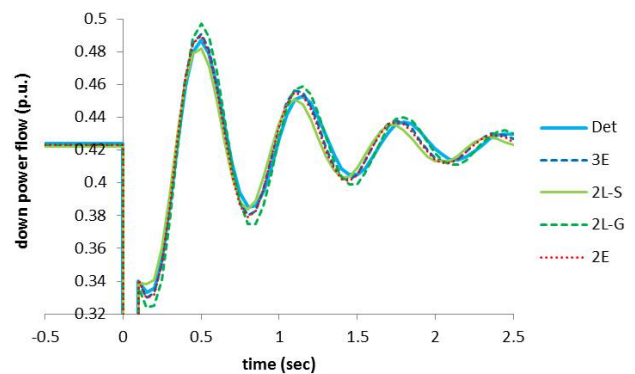


Fig. 3.8 Aggregation accuracy (static load)

In case of induction motor load, significant difference by aggregation method is seen just after fault clear. Downward flow is larger in two-element and two-load-S methods, is slightly large in two-load-G method, and small in three-element method and detailed system. When motor is accelerating from low speed due to fault, much power is claimed. The tendency appears more strongly than reality in two-element and two-load-S methods in

which impedance from aggregation point to load $Z_S + Z_{SL}$ becomes very small value. In case of static load, deceleration of motor does not exist from the beginning, and so difference by aggregation method is not significant.

RMS error of V, P, Q of initial power flow at aggregation point is defined as “flow RMS error”, and RMS error of downward power flow by 0.05 sec sampling time from fault clear (0.1 sec) to 2.5 sec is defined as “swing RMS error”.

For every aggregation method, flow RMS error (Flow), swing RMS error by induction motor load (Sw (IML)), swing RMS error by static load (Sw (St.L)) are compared in Fig. 3.7. Flow RMS error is sufficiently small (0.001 or less) in three-element method (3E), but considerable error is seen in the other methods (2L-S, 2L-G, and 2E). In case of static load, no significant difference by aggregation method on swing RMS error are seen. However in case of induction motor load, swing RMS error is small in three-element method, but large in two-load-G method, and vary large in two-load-S and two-element methods. The result agree with the analysis that impedance from aggregation point to load $Z_S + Z_{SL}$ is very smaller than reality in the two aggregation methods.

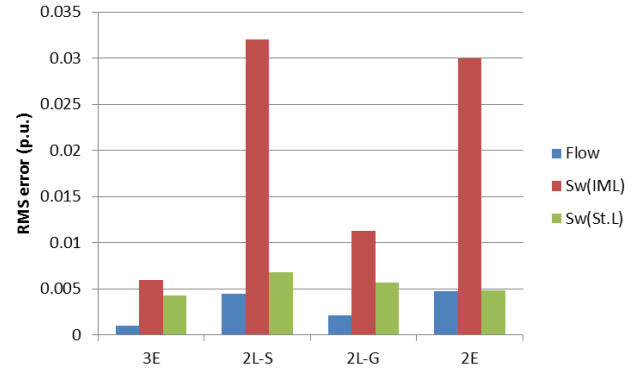


Fig. 3.7 RMS error of each aggregation method

Aggregation of generator and control system

Generator As to generator reactance, reciprocal number is preserved. Because generators connect in parallel, therefore, synthesized admittance must be preserved.

As to generator time constant, reciprocal number is preserved. Since it is resistance R under given reactance X , it is rational to preserve weighted average of reciprocal number of time constant $1/T = R/L$.

As to no-load saturation, weighted average of p.u.-field currents at 0.5, 0.8, 1.0, 1.1, 1.2 p.u.-voltage is preserved.

Frequency response of average excitation system

The frequency response affects oscillatory stability very much. Frequency response of individual excitation system and weighted average response can be conceptually expressed as Fig. 3.8. Independent parameters are the four: Low frequency gain G_L , middle frequency gain G_M , turn-over angle frequency $1/T_M$, and roll-off time constant T_H . Since T_M is slower than power swing, not time constant but angle frequency $1/T_M$ is preserved. Thus, it is avoided that few large T_M s become dominant in weighted average.

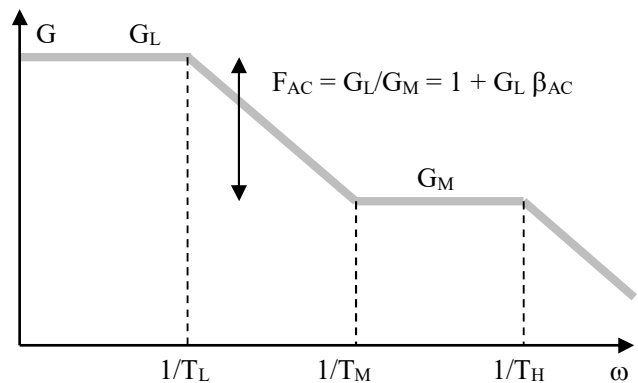


Fig. 3.8 Conceptual frequency response of excitation system

For example parameters on gain-frequency response of AC exciter type excitation system shown in 3.9 are identified. Since T_1 and T_2 ($T_2 > T_E$) are far larger than 1 sec, T_1/T_2 is incorporated into low frequency gain G_L .

$$G_L = G_A (T_1/T_2) G_E \quad \beta_{AC} = H_{AC}/T_{AC}$$

$$F_{AC} = 1 + G_L H_{AC}/T_{AC} \quad G_M = G_L/F_{AC}$$

$$T_L = F_{AC} T_M \quad T_H = (T_E + T_A) / F_{AC}$$

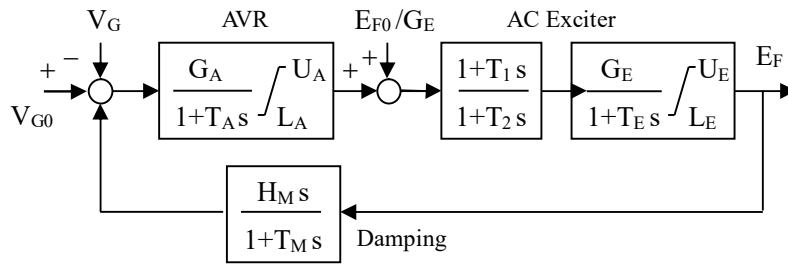


Fig. 3.9 Block diagram of AC exciter type excitation system

Speed and ceiling of average excitation system

Speed affects transient stability very much. AVR has

limiter U_A and $-L_A$, by which time the time that excitation voltage rise/dive by 1 p.u.: T_{RISE}/T_{DIVE} are calculated as follows.

$$T_{RISE} = T_E G_E / (T_1/T_2) / U_A \quad T_{DIVE} = T_E G_E / (T_1/T_2) / L_A$$

Output voltage is limited by exciter’s ceiling voltage U_E and minimum voltage $-L_E$. Although fast excitation in thyristor excitation system is positively evaluated, excitation power source is transformer connected to generator terminal (self-excitation), and so, power source voltage is reduced during and just after fault by reduced generator terminal voltage. Therefore in case of mixture of self-excitation and independent-excitation, if aggregated excitation system is modeled as independent-excitation system, transient and voltage stability will be assessed optimistically.

By simulation result, excitation voltage during 0.06 sec fault is far lower than ceiling voltage, and rises only to 90% of ceiling voltage at just after fault clear. Therefore, ceiling voltage U_E of thyristor excitation system is here evaluated as 90% of exciter type. Also thyristor type’s T_{RISE} is here evaluated as 0.1 sec. Verification of these evaluation will be done examples later.

Design of aggregated excitation system (part 1)

Exciter type with DC feedback as shown 3.10 is

assumed. Relationships between constants and parameters above mentioned are expressed as follows.

- 1) $G_L, T_A, U_E, -L_E$ are equal to average excitation system.

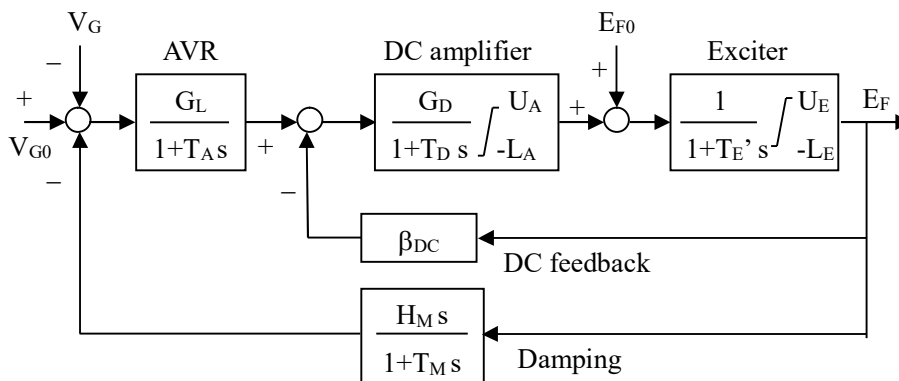


Fig. 3.10 Structure and constants assumed in aggregated excitation system (part 1)

- 2) Upper and lowest limit of DC amplifier is decided as follows. T_D is chosen as 0.01 sec, which is the minimum time constant permitted by simulation.

$$U_D = \text{Max} \{ (T_E - T_D) / T_{\text{RISE}}, U_E - 1 \} \quad L_D = U_D T_{\text{RISE}} / T_{\text{DIVE}}$$

The first term of U_D 's maximum value makes rising time $T_{\text{RISE}} = (T_E - T_D) / U_D$. Then, $T_E' = T_E - T_D$.

The second term of U_D 's maximum value is condition for generating ceiling voltage. Exciter's maximum voltage is $U_D + E_{F0} > U_E$. While Minimum value of E_{F0} is 1, ceiling voltage can be generated if $U_D > U_E - 1$. Then $T_E' = U_D T_{\text{RISE}}$. If the first term of maximum is working, the condition becomes to $T_E' = T_E - T_D$, therefore, the condition equation can be applied to both.

3) DC feedback gain β_D is tuned so that all over gain of feedback system consists of DC amplifier, exciter, feedback becomes 1. Thus, $G_D / (1 + G_D \beta_D) = 1$, so, $\beta_D = (G_D - 1) / G_D$ である。

DC amplifier gain G_D is decided so that T_H is realized. Thus, $T_H G_L / G_M - T_A = (T_E' + T_D) / G_D$, so, $G_D = (T_E' + T_D) / (T_H G_L / G_M - T_A)$ である。

4) Damping time constant T_M is that of frequency response. Feedback gain is decided as follows.

$$H_M = T_D (G_L / G_M - 1) / G_L$$

Thus, aggregated excitation system is designed.

As an example in Kyushu-S system, frequency response of designed aggregated excitation system and weighted vector average gain of individual system are compared in Fig. 3.11. In frequency of major power swing: 0.3 to 0.5 Hz, gain is well tuned, but angle is a little delayed in aggregated system. Although error can be reduced by cut and try, forward calculation only is convenient for coding, so cut and try is not performed here.

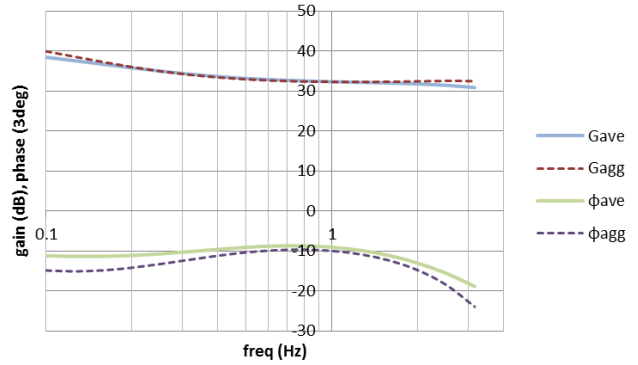


Fig. 3.11 Frequency response of excitation system 'Kyushu-S)

Design of aggregated excitation system (part 2)

Thyristor type excitation system as Fig. 3.12 is assumed. It is adopted when generators to be aggregated mainly consist of thyristor excitation.

Relationships between constants and parameters mentioned above are expressed as follows.

1) $G_L, T_A, -L_E$ are same of weighted average excitation system.

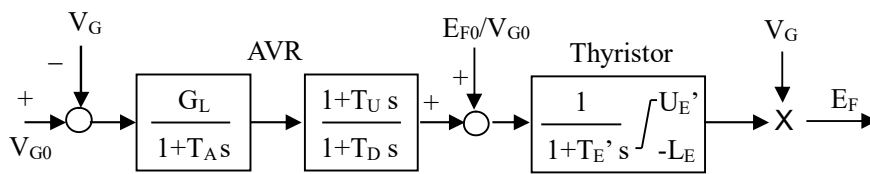


Fig. 3.12 Structure and constants assumed in aggregated excitation system (part 2)

2) Time constants of AVR and thyristor are decided as follows. Sum of the two is equal to T_H , and both must not be less than 0.01 sec.

$$T_E' = \text{Max} \{ T_H - T_A, 0.01 \} \quad T_A = \text{Max} \{ T_H - T_E', 0.01 \}$$

3) Lead and lag time constant in AVR is decided as follows.

$$T_U = T_M \quad T_D = T_M G_L / G_M$$

4) Ceiling voltage U_E' is decided as 1/0.9 of U_E calculated in part 1.

$$U_E' = U_E / 0.9$$

Thus, thyristor type aggregated excitation system is designed.

Average PSS Structure

shown in Fig. 3.13 is assumed for PSS ($\Delta P + \Delta \omega$ type).

Since speed deviation $\Delta \omega$ is integrated generator's output decrease $-P_G$ by unit inertia constant M , signal of $\Delta \omega$ type is very small at high frequency. Therefore, small delays and compensations can be

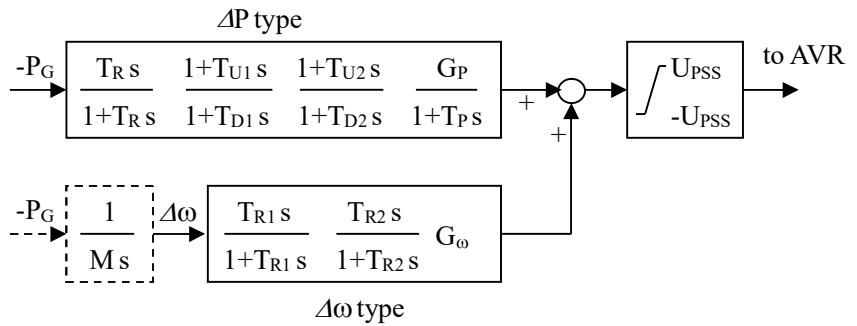


図 3.13 PSS に仮定する構造

ignored. In ΔP type small delay and two steps of compensation are modeled. The first step is lagging and the second leading. The third step is taken into the first or the second. In low frequency $\Delta \omega$ type is dominant. In high frequency ΔP type is dominant. Therefore, reset filter of $\Delta \omega$ type is modeled as T_R .

Weighted average by PSS-equipped generator capacity of $1/T_R, T_{U1}/T_{D1}, T_{D1}, T_{U2}/T_{D2}, T_{D2}, T_P$ are preserved.

Weighted average by all generator capacity of G_P, U_{PSS} are preserved.

Gain-frequency response of PSS is conceptually expressed as Fig. 3.14.

Here, ω_C is the angle frequency where $\Delta \omega$ dominant (low frequency) turns to ΔP dominant (high frequency), and relationships as follows exist. Here, M is unit inertia constant of generator.

$$G_\omega / (M \omega_C) = G_P \quad \therefore 1/\omega_C = G_P M / G_\omega$$

Transfer function at the lowest frequency is expressed as follows.

$$\frac{T_{R2} s}{1 + T_{R2} s} \frac{G_\omega}{M s} = \frac{T_{R2} G_\omega / M}{1 + T_{R2} s}$$

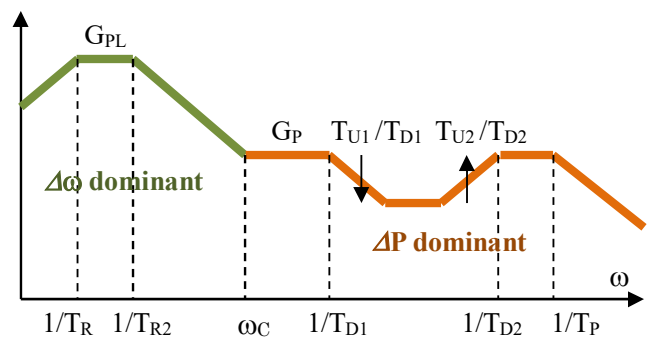


Fig. 3.14 Conceptual gain-frequency response of PSS

Inertia M is around 8 sec in large synchronous generator. Damping D certainly exist but 1 or less in inter-system slow power swing, so ignored here and rotating part is only integral $M s$ is modeled. Here, two stage reset filter is assumed in $\Delta \omega$ type. If reset filter is only one stage, its time constant is adopted as T_{R2} , and very large time constant is adopted as T_{R1} .

Design of aggregated PSS

Thus, aggregated PSS can be designed as ΔP type with three stage phase compensation. Values of $T_R, T_{D1}, T_{D2}, T_P, G_P$ are same of average PSS.

$$\begin{aligned} T_{U1} &= T_{D1} \text{Average}(T_{U1}/T_{D1}) \\ T_{U2} &= T_{D2} \text{Average}(T_{U2}/T_{D2}) \\ T_{U3} &= 1/\omega_C = G_P M / G_\omega \quad T_{D3} = T_{R2} \\ G_{PSS} &= G_{PL} = G_P T_{3D} / T_{3U} \end{aligned}$$

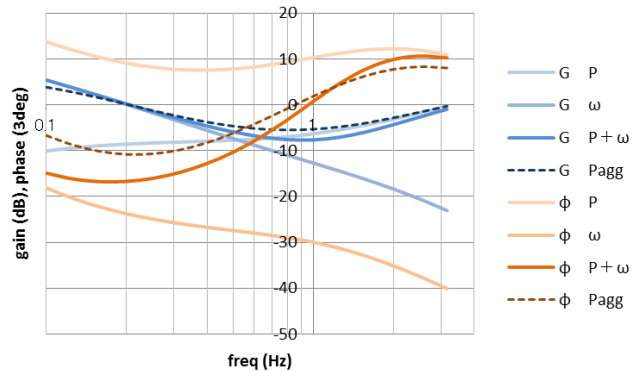


図 3.15 $\Delta P + \Delta \omega$ 型 PSS の周波数特性の一例

By study above, $\Delta P + \Delta\omega$ type PSS can be replaced by equivalent ΔP type PSS. Fig. 3.15 is frequency response of a $\Delta P + \Delta\omega$ type PSS, which can be replaced by ΔP type. Certainly in 0.4Hz or lower frequency $\Delta\omega$ type is dominant and in 0.5Hz or higher frequency ΔP type is dominant.

The replaced ΔP type PSS can be described as Fig. 3.16. A large lagging compensation exists as the third stage, and gain at low frequency is considerably large. There exists a possibility that economical ΔP type can replace expensive $\Delta P + \Delta\omega$ type.

$$\frac{2s}{1+2s} \frac{1+0.22s}{1+0.26s} \frac{1+0.15s}{1+0.02s} \frac{1+0.3108s}{1+5s} \frac{6.345}{1+0.015s} \int_{-0.05}^{0.05}$$

Fig. 3.16 Transfer function of ΔP type replaced $\Delta P + \Delta\omega$ type

Thus aggregated PSS is designed.

As an example, frequency response of vector average by generator capacity of individual PSS and that of aggregated PSS are shown in Fig. 3.17. Around 0.3 to 0.5Hz power swing frequency of major power swing, around 1 dB error in gain and 6 deg error in angle are seen. Likely excitation system, these error can be reduced by cut and try. Although error can be reduced by cut and try, forward calculation only is convenient for coding, so cut and try is not performed here.

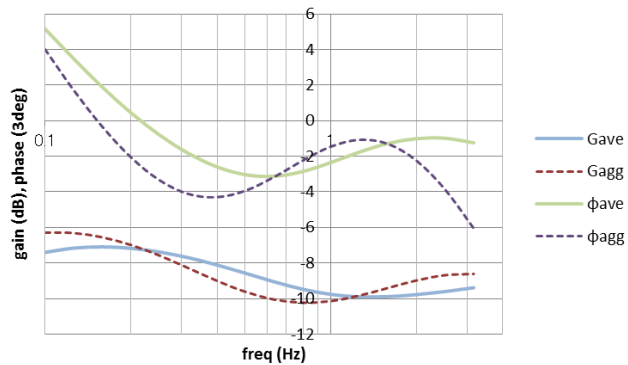


Fig. 3.17 Frequency response of average and aggregated PSS

Parameters of average governor Governor’s character is quite different in hydro and thermal. Therefore, classified in some frequency region. As very slow time constant around 10sec, elastic return in hydro and reheater in thermal exist and they can be treated same.

As a little faster elements around 1 sec, water hammering in hydro exists. This is a troublesome element in control that shows 200% gain with 180 deg. phase lagging at higher frequency. In thermal corresponding element does not exist, but second largest time constant of HP turbine is regarded as mitigating water hammering.

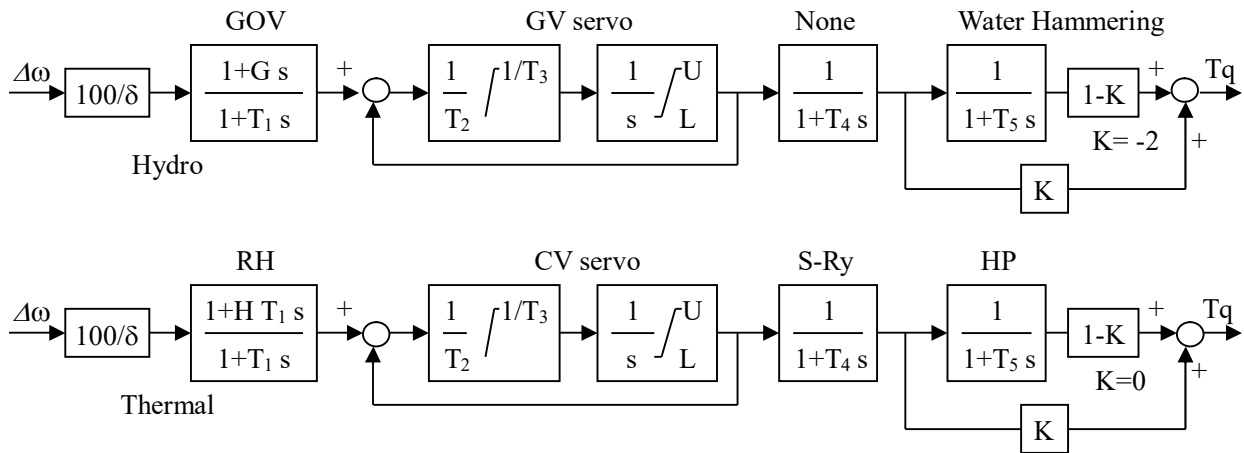


Fig.3.18 Correspondence of hydro and thermal elements in speed governing system

In Fig. 3.18, correspondence between hydro and thermal turbines are shown.

Hydro governor includes elastic return (T_1 is 5 to 40 sec, G is around 30% of T_1). In corresponding thermal governor, reheater with around 10 sec time constant and high pressure turbine with around 0.3 sec time constant.

Guide vane (GV) in hydro corresponds to control valve (CV) in thermal. T_2 is around 0.2 sec and T_3 is around 7 sec in both hydro and thermal.

T_4 around 0.12 sec means speed relay in thermal. In hydro, corresponding element does not exist and T_4 is set as very small (0.01 sec).

T_5 means water hammering in hydro. In thermal, high pressure (HP) turbine time constant (around 0.3 sec, $K = 0$) is represented.

Design of aggregated governor In aggregation, generator (including load limiter operation) rated output weighted average value of $100/\delta$ is preserved. Generator (only governor free operation) rated output weighted average values of K , T_1 , T_2 , $1/T_3$, T_4 , T_5 , U , L , G are preserved.

Fig. 3.19 compares frequency response of weighted average speed governor and aggregated speed governor in Kyushu-S system, in which hydro, thermal, and nuclear are mixed. Gain is almost preserved. But phase lagging is larger in aggregated than average. That means aggregation will show somewhat pessimistic result.

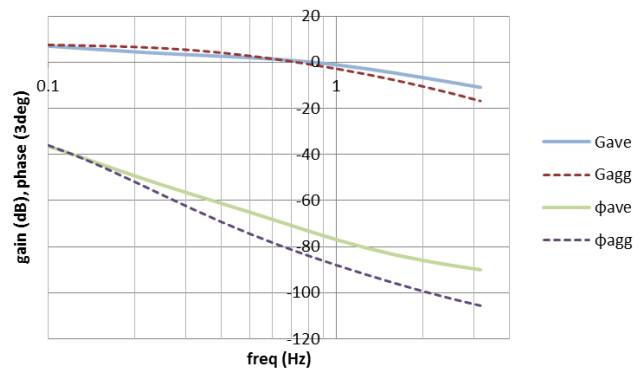


Fig 3.19 Comparison of average and aggregated governor

Aggregation examples in trunk system

A system in 2008 when trunk system expansion is not finished are taken as example. Detailed system with 28 generators and 30 loads are shown in Fig. 3.20, and aggregated system with 6 generators and 4 loads is shown in Fig. 3.21.

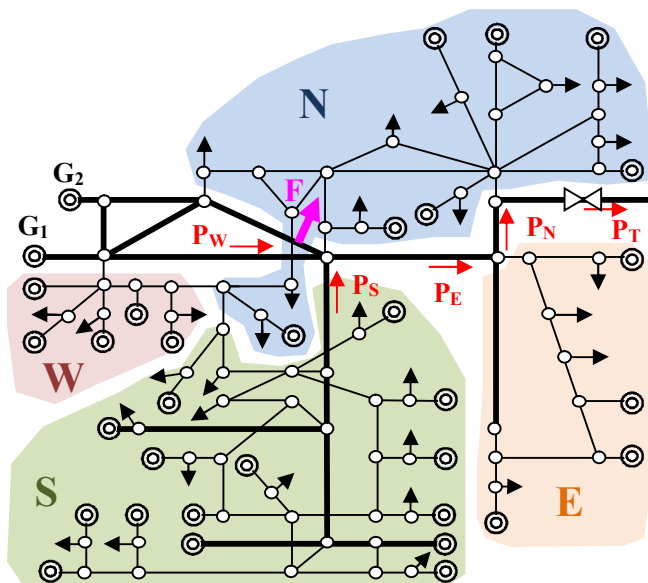


Fig 3.20 Detailed Kyushu system in 2008

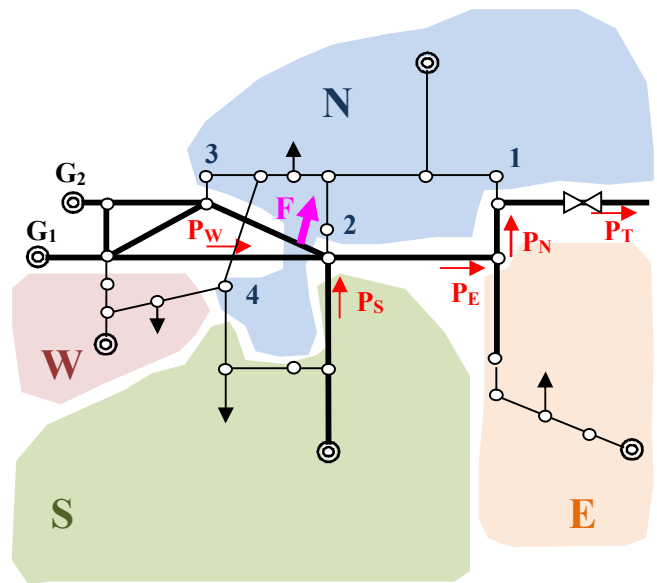


Fig. 3.21 Aggregated Kyushu system in 2008

Induction motor load (50% motor ratio, 50% loading, and 0.5 sec inertia) and load branch impedance (66kV bus to load) are modeled.

Trunk power source G1 and G2 is not aggregated for observing angle swing.

The other parts: S, E, W, and N are baldly aggregated to one machine and one load.

S and W have two interconnection, and E has one. Y-connection aggregation method is applied.

N has four interconnection. As between them, Z_{12} between 1 and 2, Z_{23} between 2 and 3, and Z_{34} between 3 and 4 are preserved, but the others are let taken natural courses. Structure of aggregated system is compared as character “H”, and the four interconnection correspond the four tiptoos. Load is located at midst of central lateral bar. Thus the four interconnection have the same position.

Aggregation accuracy is assessed by error on trunk power flow P_W , P_S , P_E , P_N and tie line power flow P_T .

Aggregation accuracy As failure, one circuit 3LG-O on double circuit 500kV transmission line at F is modeled. Clearing time is 0.06 sec. If 0.07sec, synchronism is lost, because partial load drop due to voltage sag is ignored. Considering the load drop, stability is maintained. Here, load drop is ignored for simplicity. Ten second simulation is held. Accuracy is assessed by RMS error of every 0.1 sec on trunk power flow P_W , P_S , P_E , P_N , P_T shown in Fig. 3.20 and 3.21.

Simulation result by the proposed aggregation method is shown in Fig. 3.22. Lines of aggregated system almost pile up to lines of detailed system. Such accurate trunk system aggregation was ever not seen.

As to loss preservation, tie line sending power is 1590MW in both detailed and aggregated system. 1MW error does not appear. Total sending power of generators is 19,212MW, sum of load power and tie line sending power is 18,932MW. Therefore, network loss is 280MW. 1MW error is 0.005% of generator sending power, and is 0.36% of loss. The accuracy is sufficient.

RMS error of the five trunk power flow is 344MW. This is 4.4% of maximum tie line power variation width (5051MW to -2739MW). It is sufficient accuracy for oscillatory stability.

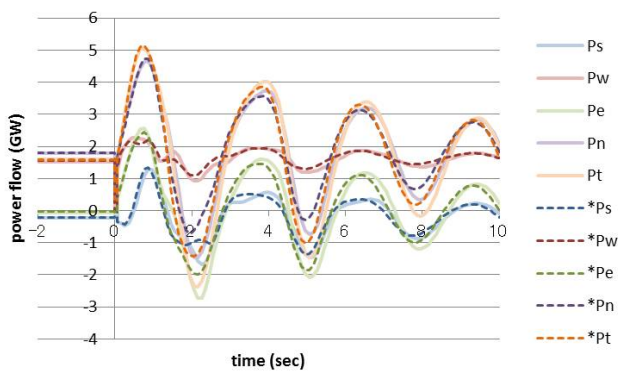


Fig. 3.22 Five trunk power flows by proposed aggregation

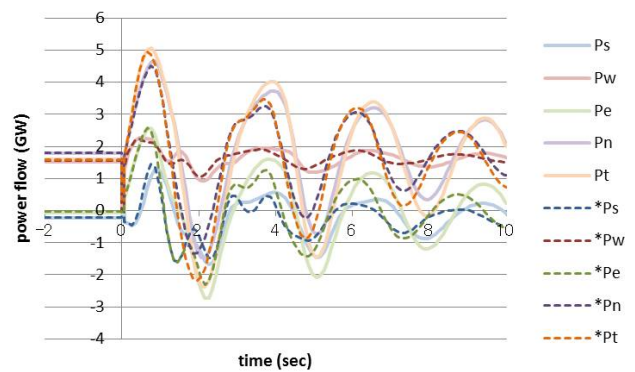


Fig. 3.23 By control system of the largest generator

Representing by the largest generator’s control system In system aggregation function of simulation tool used in practice up to now, control system of aggregated generator is represented by that of the largest generator included in detailed system to be aggregated. The method is somewhat rough, so accuracy decline by the approximation is assessed here. The result is shown in Fig. 3.23. Aggregated system shows shorter period and smaller amplitude than detailed system. Since the largest generator must be a modern high-spec machine, oscillatory and transient stabilities must be better than usual machine. That is, aggregated model employing the

largest generator’s control system must bring a risk to assess system stability optimistic unreasonably.

Connecting load to 66kV class bus directly

1) In system aggregation function of simulation tool used in practice up to now, aggregated load is directly connected to 66kV class bus.

2) Also in IEEJ standard power system model, transformer to 66kV class is considered, but impedance under 66kV class bus is not considered.

These are clearly different from reality, so accuracy decline by connecting load direct to 66kV class bus is assessed here. For compensating decrease of loss, imaginary constant impedance load is added and initial power flow is preserved.

The result is shown in Fig. 3.24. In direct connection case, shorter period and smaller amplitude than detailed system like largest generator’s control system case.

Summing up of trunk system 各 RMS errors on the five trunk power flow by the three aggregation methods during simulation time are compared in Fig. 3.25. Largest generator’s control system case (MaxG) and connecting load to 66kV class bus directly case (woZL) shows quite inferior aggregation accuracy than proposed method (Agg), as easily judged by power swing of the three simulation results.

Time sequential tie line power flow variation of detailed system and every aggregated system are compared in Fig. 3.26. Proposed method (Agg) well agrees with detailed system (Det) except that first and second minus side amplitude are slightly smaller. Largest generator’s control system case (MaxG) and connecting load to 66kV class bus directly case (woZL) show quite optimistic result unreasonably.

Thus it must be noticed that large aggregation error appears without employing the proposed method, when aggregating detailed system modeling induction motor load and load branch.

Transient stability Fault clearing time is

extended to 0.07 sec. The result are shown in Fig. 3.27.

Detailed system (Det) is slightly unstable than critical. Proposed aggregation shows slightly inn stability than

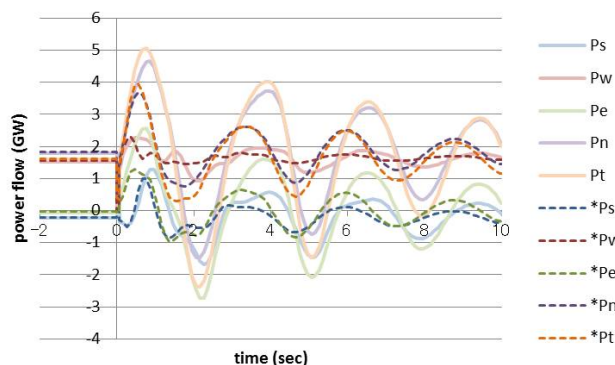


Fig 3.24 Connecting load to 66kV class bus directly

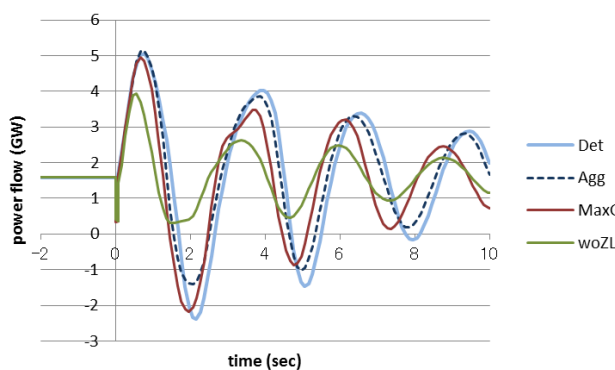
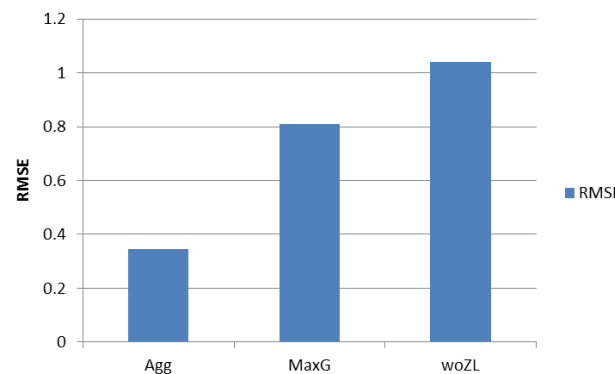


Fig. 3.26 Tie line power swing by aggregation method

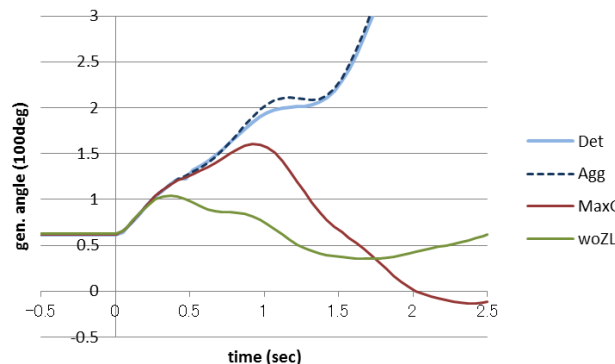


図 3.27 縮約法による過渡安定度の相違

detailed system. Largest generator's control system case (MaxG) shows quite well stability. Connecting load to 66kV class bus directly case (woZL) shows more better stability than the former case.

Also here it must be noticed that large aggregation error appears without employing the proposed method, when aggregating detailed system modeling induction motor load and load branch.

Proposed aggregation method (Agg) shows slightly ill stability than detailed system (Det). This is Favorable for screening function. As the result it is found that discounting ability of thyristor type excitation system was adequate.

References

- (1) "Power System Stability", Co-research on Electric Power, Vol. 34, No. 5, p.25 (1979)
- (2) Geeces: "A Modal-Coherency Technique for Deriving Dynamic Equivalents", IEEE Tran. on Power Systems, Vol. 3, No. 1, , pp. 44-51. (Feb. 1988)
- (3) Liyanage, Yokoyama, Sekine: "Coherency for Power System through Modal Analysis —From Perfect to Close Coherency—", T. IEE Japan, Vol. 111-B, No. 8, pp. 850-858 (1991)
- (4) Trudnowski: "Order Reduction of Large-scale Linear Oscillatory System Models", IEEE Trans. on Power Systems, Vol. 9, No. 1, pp. 451-458, (Feb. 1994)
- (5) de Oliveira, de Queiroz: "Modal Dynamic Equivalent for Electric Power Systems", IEEE Tran. on Power Systems, Vol. 3, No. 4, pp. 1723-1737, (Nov. 1988)
- (6) Newell, Risan, Allen, Rao, Stuehm: "Utility Experience with Coherency-Based Dynamic Equivalents of Very Systems", IEEE Tran. on Power Systems, Vol. PAS-104, No. 11 pp. 3056-3063, (Nov. 1985)
- (7) Price, Hurysz, Chow, Hirsch: "Large-Scale Testing of a Power System Dynamic Equivalencing Program", IEEE Trans. on Power Systems, Vol. 13, No. 3, pp. 768-774, (Aug. 1998)
- (8) Mansour, Vaahedi, Chang, Corns, Garret, Demaree, Athary, Cheung: "B. C. Hydro's On-Line Transient Stability Assessment(TSA) Model Development, Analysis and Post-Processing", IEEE Trans. on Power Systems, Vol. 10, No. 1, pp. 241-253, (Feb. 1995)
- (9) Yusof, Alden, Rogers: "Slow Coherency Based Network Partitioning Including Load Buses", IEEE Trans. on Power Systems, Vol. 8, No. 3, pp. 1375-1382, (Aug. 1993)
- (10) Yamagishi, Komami: "Practical Power System Aggregation Considering Dynamic Loads", IEEJ Trans. on PE, Vol. 128, No. 2, (2008)
- (11) Yamagishi, Hosoki, Komami, and Mizukami: "A Study on Power System Aggregation Including Induction Motor Load", IEEJ Annual Conference, No. 230 (2002)
- (12) S. Komami and T. Sakata: "Power System Aggregation Considering Insuction Motor Load and Network Path to Load", IEEJ Annual Conference PE, No. 17 (2016)
- (13) Y. Inoue: "A study on Reduction of Power System", IEEJ Proc. IP, IP-75-23 (1975)
- (14) McCalley, Dorsey, Luini, Mackin, Molina: "Subtransmission Reduction for Voltage Instability Analysis", IEEE Trans. on Applied Super- conductivity, Vol.3, No.1, ,pp.349-356 (March 1993)